Electronic Supplementary Material for Journal of Materials Chemistry A.

Supplementary Information

Recognizing chiral amino acids with a dual-optical-response system

Yaxin Wang[#], Yajie Zhou[#], Shanshan Zhao, Mingjiang Zhang, Anqi Li, Guangen Li, Qi Guo, Xueru Guo, Zhi Tong, Zeyi Li, Jing Lin, Taotao Zhuang*

Department of Chemistry, Division of Nanomaterials and Chemistry, Hefei National Research Center for Physical Sciences at the Microscale, University of Science and Technology of China, Hefei 230026, China

*Corresponding Author: Taotao Zhuang, Email: tzhuang@ustc.edu.cn

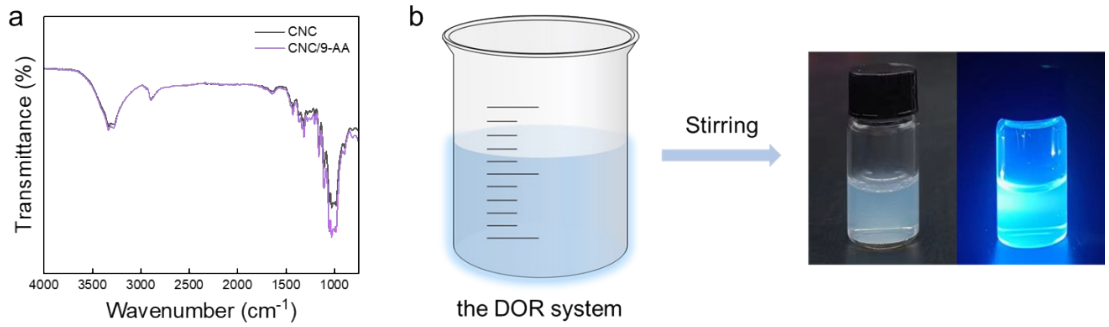

Figure S1 (a) Fourier transform infrared spectra of CNC and the system films. (b) Images of the DOR system under indoor light (left) and UV light (right) with stirring, illustrating the uniformity of the system.

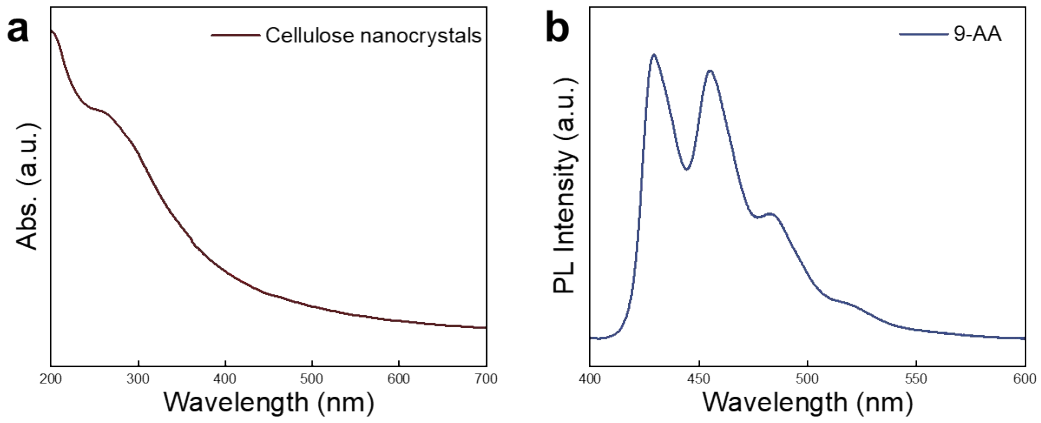

Figure S2 (a) UV–vis spectrum of cellulose nanocrystals, showing the absorption in near the ultraviolet region. (b) PL spectrum of 9-AA solution under 350 nm UV irradiation, showing blue emission.

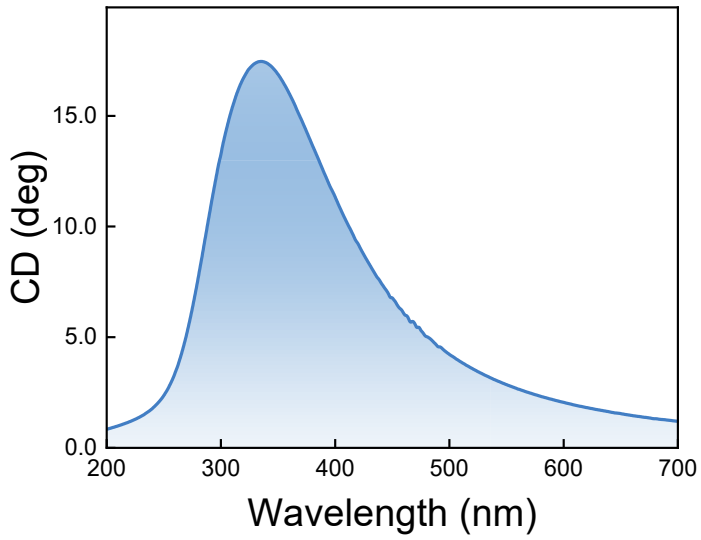

Figure S3 CD spectrum of cellulose nanocrystals, illustrating nematic organization.

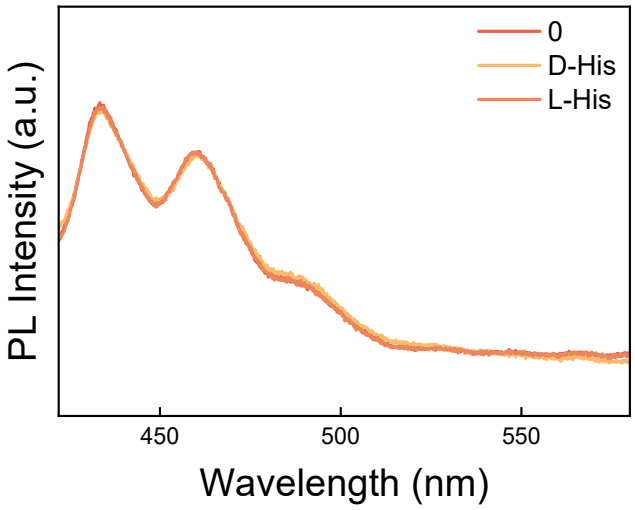

Figure S4 PL spectra of the DOR system with His at a concentration of 100 mg/mL under 350 nm UV irradiation, evidencing the fluorescence intensity maintaining of the system even with more His.

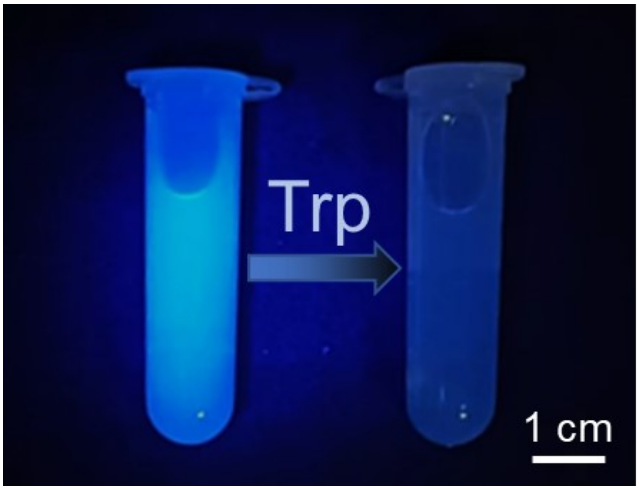

Figure S5 Photograph of the DOR system with Trp at a concentration of 15 mg/mL under 365 nm UV irradiation, showing the fluorescence quenching.

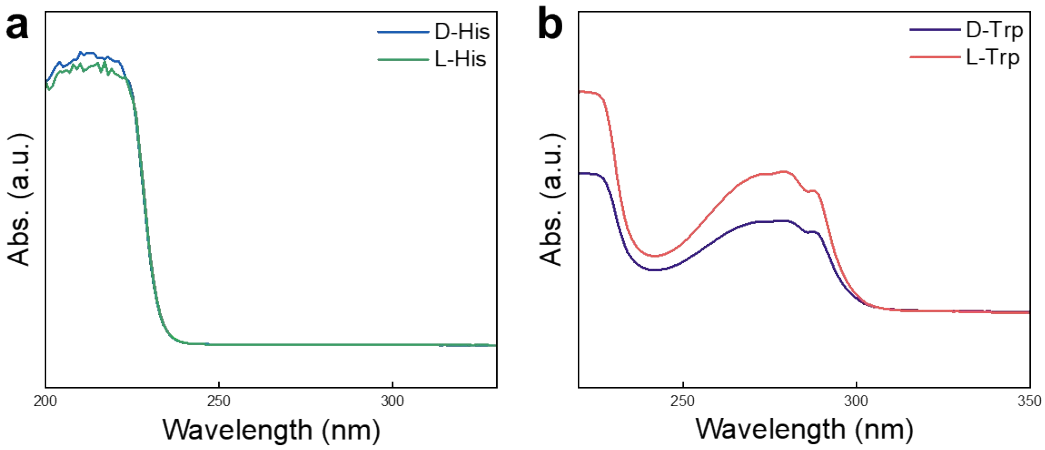

Figure S6 (a) UV–vis spectra of His and (b) Trp enantiomers, showing the maximum absorption below 300 nm.

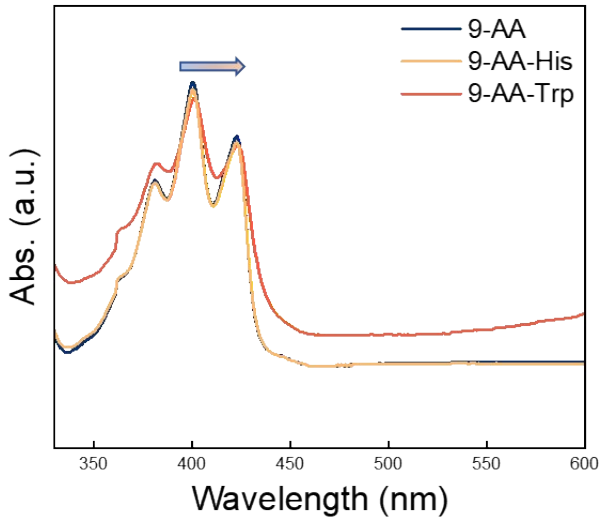

Figure S7 UV–vis spectra of 9-AA solution in the presence of His and Trp. Trp enables the redshift and decrease of peak, indicating the interaction between 9-AA and Trp [1].

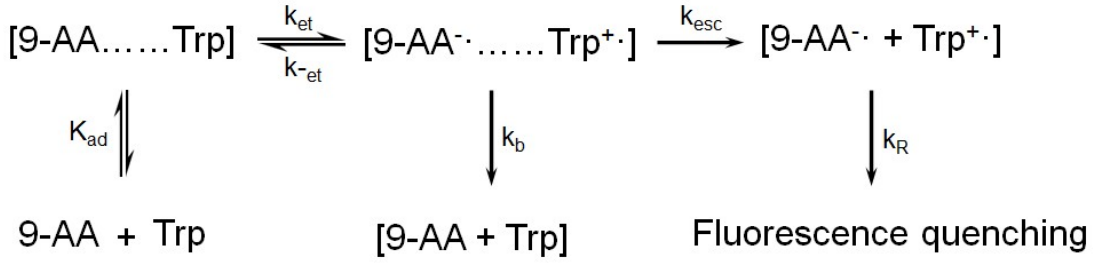

Figure S8 The fluorescence quenching of 9-AA triggered by amino acids, e.g., Trp, resulting from the electron transfer process between Trp and 9-AA.[1, 2]

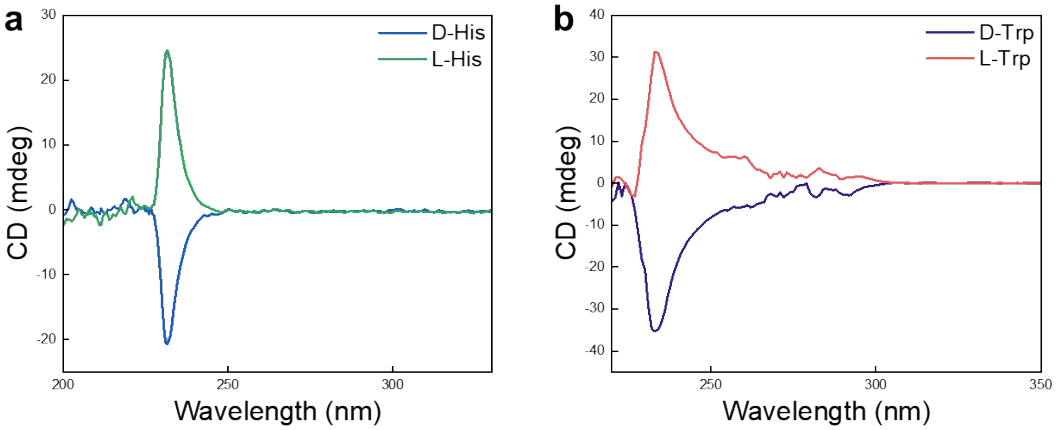

Figure S9 (a) CD of His and (b) Trp enantiomers, showing the initial chiral characteristic of these two amino acids.

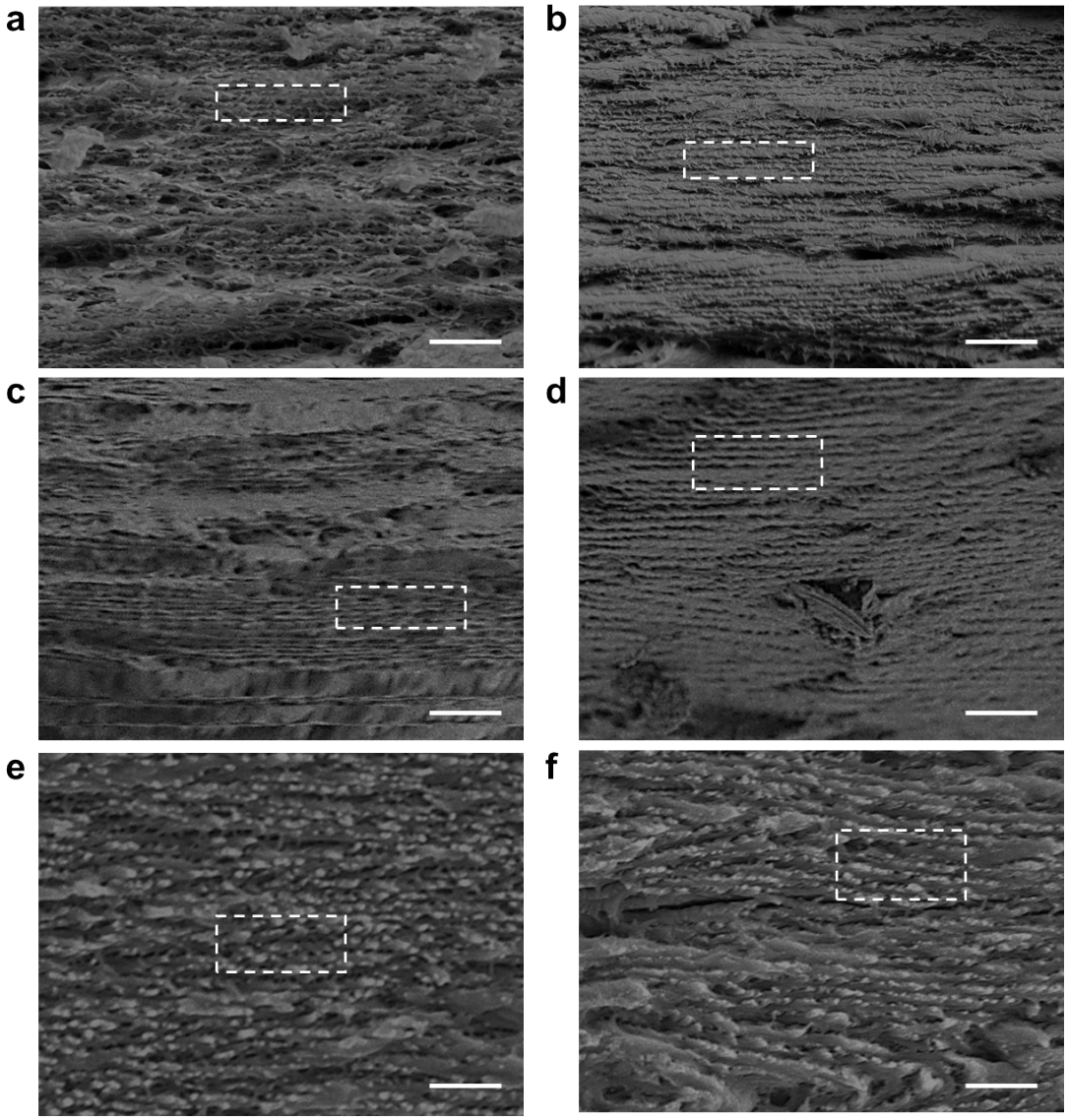

Figure S10 Cross-sectional SEM images of the DOR system in the presence of His, showing periodic layers. (a) 1 mg/mL D-His, (b) 1 mg/mL L-His, (c) 7 mg/mL D-His, (d) 7 mg/mL L-His, (e) 15 mg/mL D-His, (f) 15 mg/mL L-His. The pitch increased with the addition of His, and L-His caused larger pitches of the DOR system compared with D-types. Scale bars: 1 μm.

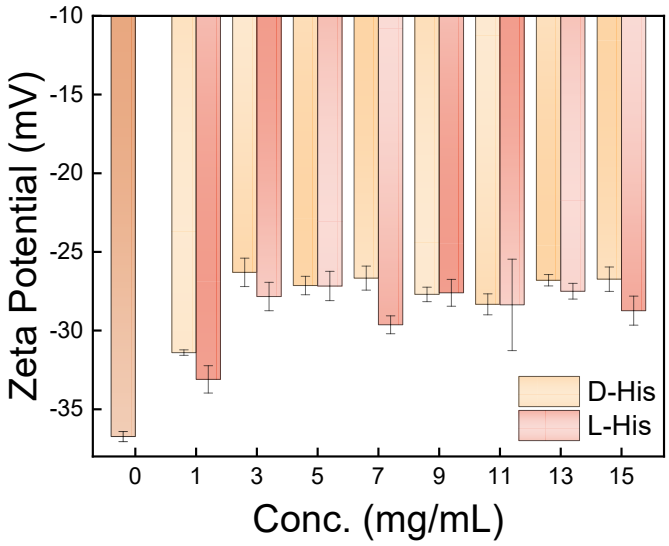

Figure S11 Zeta potential values of the DOR system in the presence of His at different concentrations, showing the reduction of charges induced by His. The error bars represent the standard deviation from the average (N = 3).

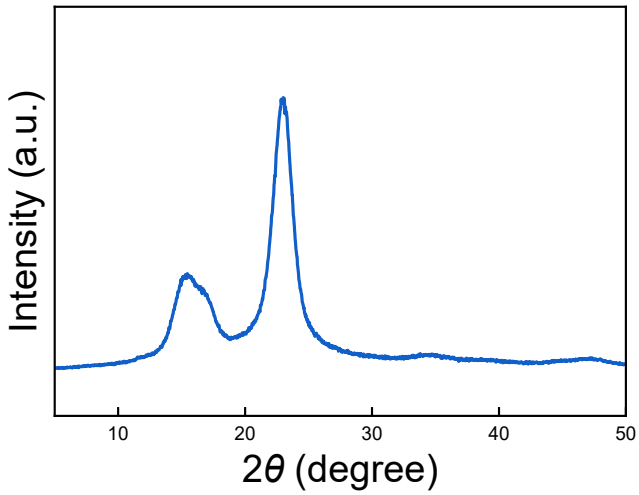

Figure S12 Powder XRD pattern of the DOR system. The diffraction pattern was recorded at 2θ = 22.78°, corresponding to the characteristic diffraction peak of cellulose nanocrystals.[3, 4]

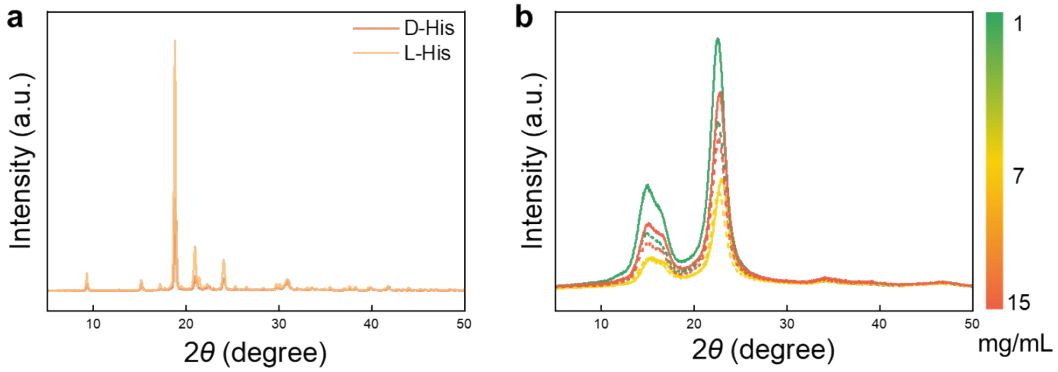

Figure S13 (a) Powder XRD patterns of His.[5, 6] (b) Powder XRD patterns of the DOR system in the presence of His. Lower crystallinity of the system induced by L-His demonstrated that L-His was more easily dispersed within the system. Solid lines correspond to D-His, and imaginal lines are about L-His. It was worth noting that the small content of amino acids caused no characteristic peaks of themselves in the XRD spectra.

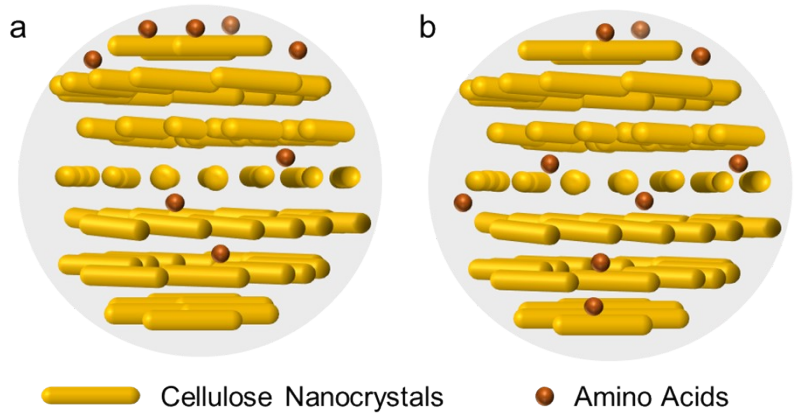

Figure S14 Schematic illustrating the dispersion of amino acid enantiomers in the CNC layers. (a) D-amino acids. (b) L-amino acids.

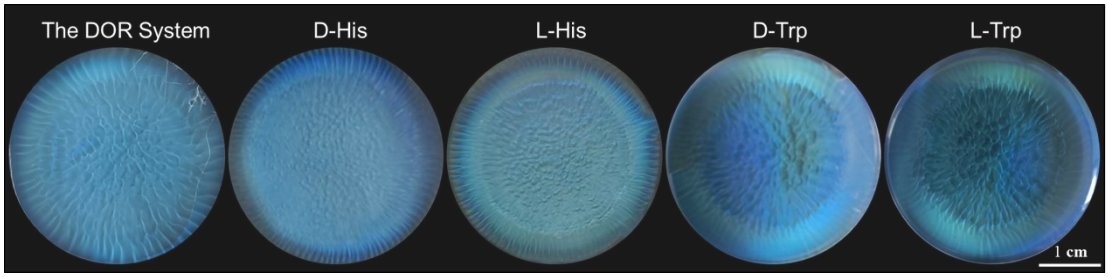

Figure S15 Photographs of the DOR system and the system in the presence of D- and L-His at 15 mg/mL and Trp at 0.05 mg/mL.

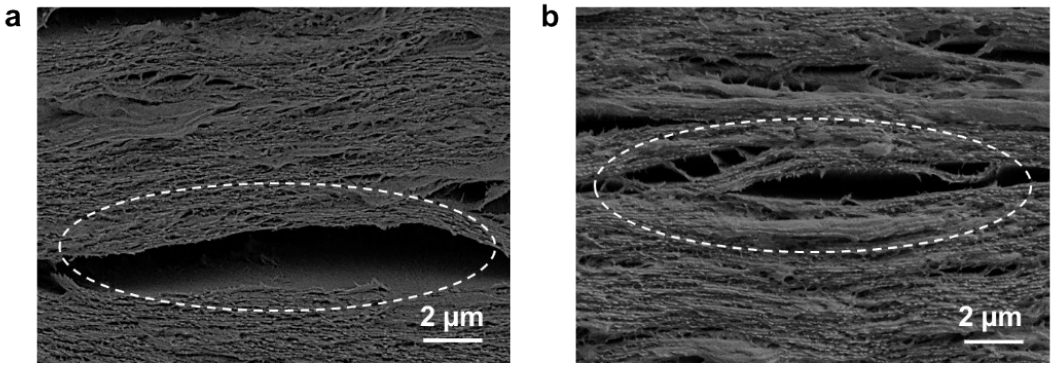

Figure S16 SEM images of the DOR system in the presence of His at the concentration of 15 mg/mL, showing hollows in the structures. (a) D-His. (b) L-His.

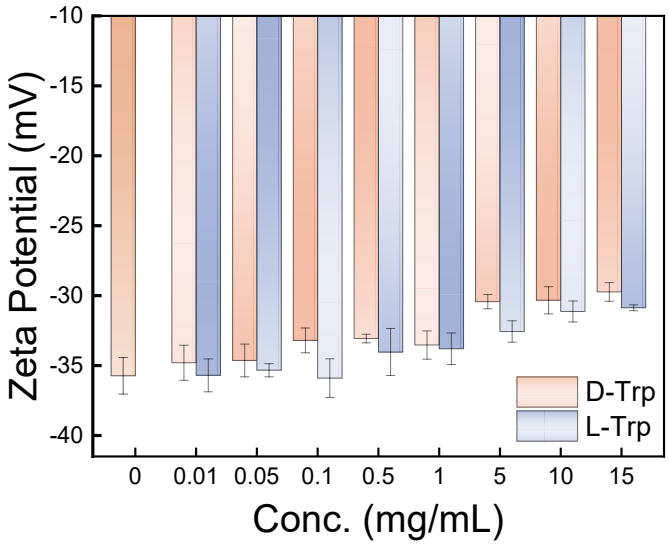

Figure S17 Zeta potential values of the DOR system in the presence of Trp at different concentrations, showing the influence of Trp on the system which reduced electrostatic repulsion of the system. The error bars represent the standard deviation from the average (N = 3).

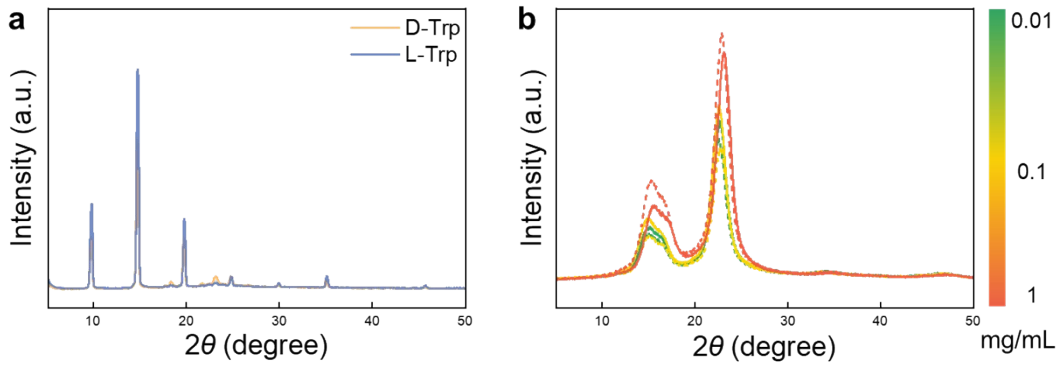

Figure S18 (a) Powder XRD patterns of Trp, agreed with the reported results.[7] (b) Powder XRD patterns of DOR system with Trp, showing L-Trp has a stronger diffraction peak at 14.76°, close to the characteristic peak of the DOR recognition system at 14.86°, indicating that it was easier to intercalate into the system than D-types. Solid lines correspond to D-Trp, and imaginal lines refer to L-Trp.

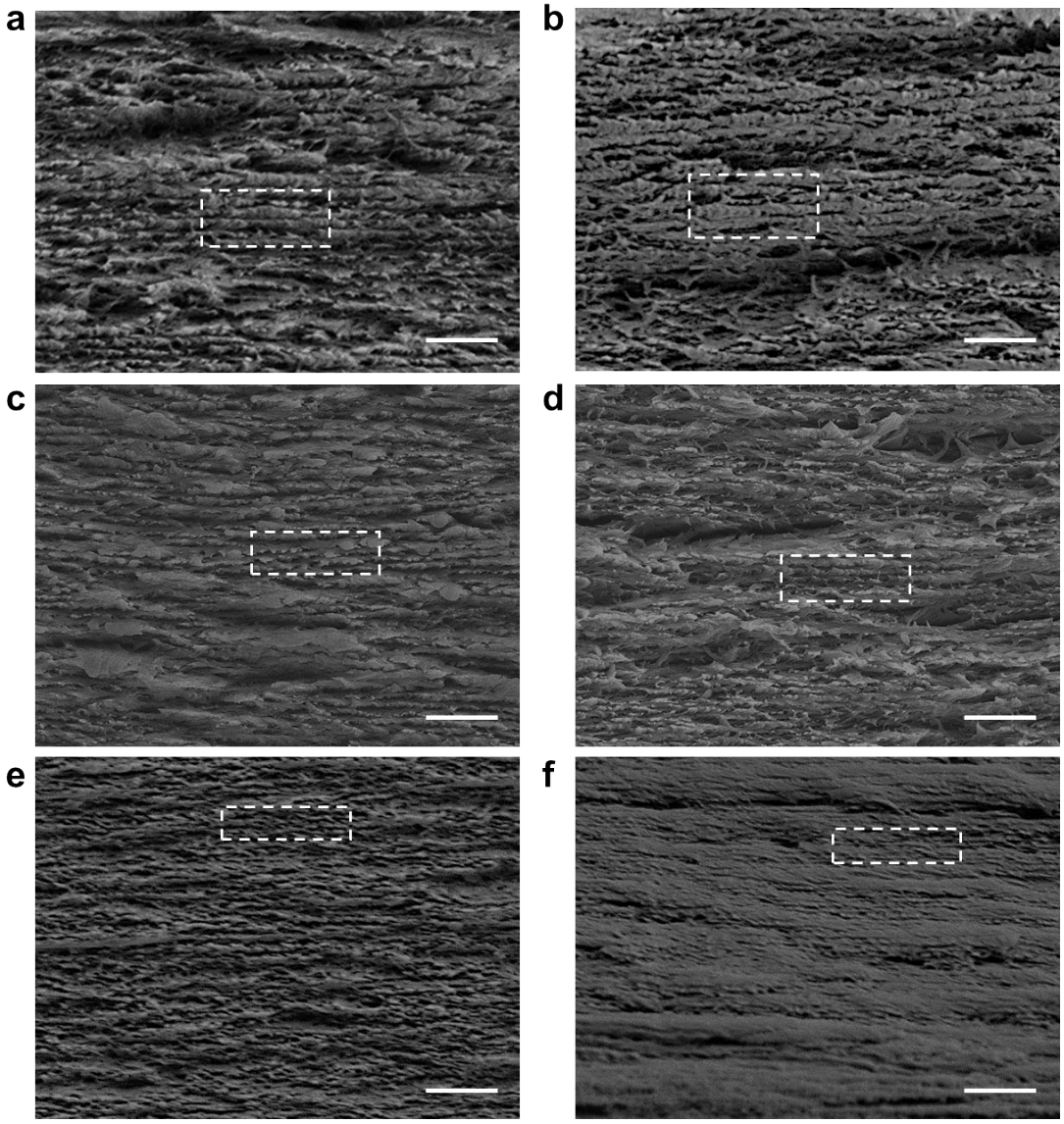

Figure S19 Cross-sectional SEM images depicting chiral nematic organization of the DOR system in the presence of Trp. (a) 0.01 mg/mL D-Trp, (b) 0.01 mg/mL L-Trp, (c) 0.1 mg/mL D-Trp, (d) 0.1 mg/mL L-Trp, (e) 1 mg/mL D-Trp, (f) 1 mg/mL L-Trp. The pitch decreased with the Trp, and the DOR system with L-Trp always exhibited a larger pitch, compared to with the addition of D-type. Scale bars: 1 μm.

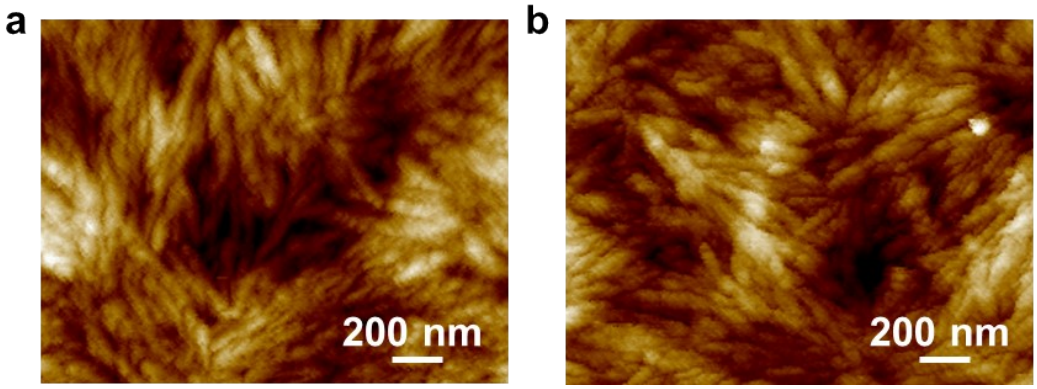

Figure S20 AFM images of the DOR system with the Trp of 1 mg/mL, showing irregular arrangement. (a) D-Trp, (b) L-Trp.[8]

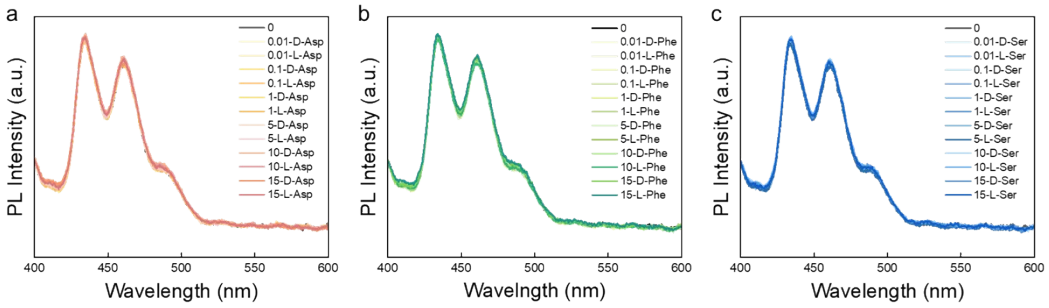

Figure S21 PL spectra of the DOR system with the addition of amino acid enantiomers at different concentrations. (a) PL spectra with aspartic acid (Asp). (b) PL spectra with phenylalanine (Phe). (c) PL spectra with Serine (Ser). The concentrations ranged from 0.01 mg/mL to 15 mg/mL.

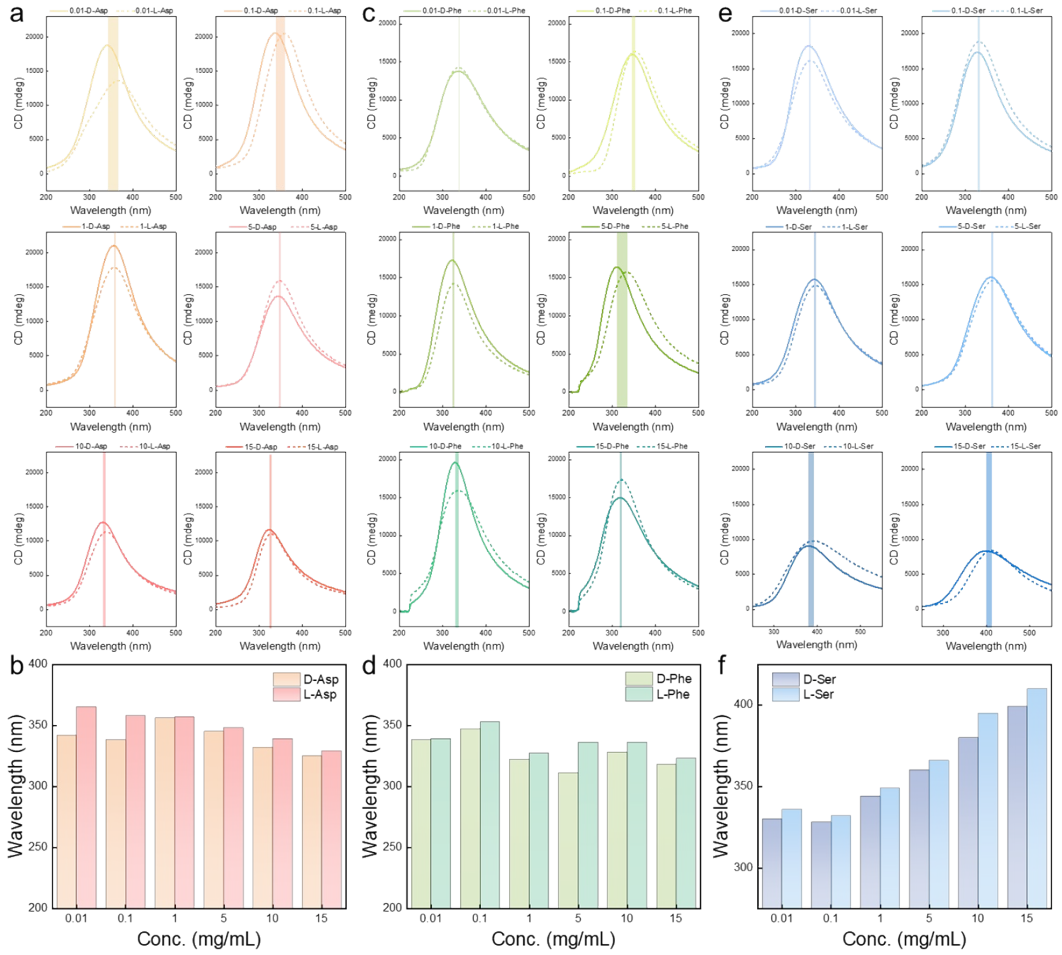

Figure R22 Peak shifts in the CD spectra of the system with other amino acids. (a) CD spectra and (b) the corresponding peak shifts of the system with the addition of Asp. (c) CD spectra and (d) the corresponding peak shifts of the system in the presence of Phe. (e) CD spectra and (f) the corresponding peak shifts of the system in the presence of Ser.

References

1 C. Manivannan, R. Renganathan, *Spectrochim. Acta A Mol. Biomol. Spectrosc*., 2011, **82**, 475-80.

2 C. Manivannan, R. Renganathan, *Journal of Lumin*., 2011, **131**, 2365-2371.

3 K. Adstedt, E. A. Popenov, K. J. Pierce, R. Xiong, R. Geryak, V. Cherpak, D. Nepal, T. J. Bunning, V. V. Tsukruk, *Adv. Funct. Mater*., 2020, **30**, 2003597.

4 J. Chen, Z. Ling, X. Wang, X. Ping, Y. Xie, H. Ma, J. Guo, Q. Yong, *Chem. Eng. J*., 2023, **466**, 143148.

5 W. Li, Y. zhu, Z. Liu, Z. Fei, H. Zhao, *Chem. Eng. Data*, 2019, **64**, 5571-5577.

6 X. Xiao, J. Chen, Z. Ling, J. Guo, J. Huang, J. Ma, Z. Jin, *Polymers (Basel)*, 2021, **13,** 4389.

7 Y. Chen, K. Zhang, Y. Bao, X. Wang, *Res. Chem. Intermed*., 2017, **43**, 4907-4921.

8 W. Ge, F. Zhang, D. Wang, Q. Wei, Q. Li, Z. Feng, S. Feng, X. Xue, G. Qing, Y. Liu, *Small*, 2022, **18** (12), e2107105.